Journal of Physics: Conference Series **244** (2010) 022060 doi:10.1088/1742-6596/244/2/022060

Fast electron propagation in high-density plasmas created by 1D shock wave compression: experiments and simulations

J J Santos[1], D Batani[2], P McKenna[3], S D Baton[4], F Dorchies[1], A Dubrouil[1], C Fourment[1], S Hulin[1], E d'Humières[1], Ph Nicolaï[1], L Gremillet[5], A Debayle[6], J J Honrubia[6], P Carpeggiani[2], M Veltcheva[2], M N Quinn[3], E Brambrink[4] and V Tikhonchuk[1]

[1] Université Bordeaux 1, CELIA, Talence, France
[2] Dipartimento di Fisica "G. Occhialini", Univ. degli Studi di Milano-Bicocca, Milan, Italy
[3] SUPA, Department of Physics, University of Strathclyde, Glasgow, UK
[4] LULI, Ecole Polytechnique - CNRS - CEA, Palaiseau, France
[5] CEA-DPTA, Bruyères-le-Châtel, France
[6] GIFI, Universidad Politécnica, Madrid, Spain

E-mail: Santos.Joao@celia.u-bordeaux1.fr

Abstract. We present results from an experimental characterization of fast electron transport in high density plasmas created by 1D shock wave compression. The Kα fluorescence from a Cu layer embedded in Al or CH foil targets is measured. We use long laser pulses (LP) with 180 J, 1.5 ns, 0.53 μm to compress the foils by shock wave propagation to 2-3 times their solid density and heat them to ~ 4 eV (close to the Fermi temperature). A counter-propagating high-intensity short laser pulse (SP), with 40 J, 1 ps, 5×10^{19} Wcm^{-2}, generates intense currents of fast electrons which propagate through the deep regions of the target just before shock breakthrough. The results are compared to the uncompressed, solid density case (without the LP beam). The complete set of measurements is compared to numerical results, including a 2D hydrodynamic description of the compression and pre-pulse effects, 2D PIC simulations of the SP beam interaction and both hybrid and PIC simulations of the electron transport in the target depth and sheaths. In the case of the non-compressed targets we need to take fast electron refluxing into account to reproduce the experimental results. By exploring the domain of warm temperatures, we identify a regime for the incident fast electron current density, $10^{10} < j_h < 10^{12}$ Acm^{-2}, for which the collective mechanisms of electron transport differs appreciably between solid density and compressed matter.

1. Introduction

In the fast ignition scheme for inertial confinement fusion, an energetic electron current, produced by an ultra-intense laser, heats a highly compressed DT plasma core. The fast electrons must transport a few 10s kJ of energy from their source, near critical density, over a few 100 μm of overdense plasma, to the high density fuel (at some 1000 times the solid density). Experiments have been successfully carried out in initially cold, solid targets to understand the mechanisms of fast electron transport in dense matter. However, in those experiments the initial target conditions are far from those expected in a fast ignition target, and fast electron propagation

will therefore probably be different under such conditions. Whilst not yet being able to reproduce the fusion target core conditions, it is important to study fast electrons transport in warm and dense plasmas [1, 2], representative either of the degeneracy of the compressed fuel or of the density and temperature levels near the fast electron source.

Planar 1D compression with a counter-propagating electron flux geometry is adopted in this work. This has the advantage of ensuring plasma homogeneity over a large region around the fast electron propagation axis, but does not enable ρr to be varied, and therefore the effects of compression on the electron collisional stopping power to be measured. This configuration is adapted to identify compression-induced changes in the collective fast electron transport mechanisms. The so-called anomalous stopping power can be a non negligible source of energy loss for the injected fast ignition electron beam, mostly in regions close to the fast electron source (after the cone tip for a cone-based target or at the edge of a density channel hole bored in the coronal plasma), where the injected electrons current density is very high. The warm and dense plasma conditions we obtained by shock propagation in foil targets, reaching densities of $\sim 5\,\mathrm{g/cc}$ and temperatures $\sim 4\,\mathrm{eV}$, are representative of the fusion target coronal plasma after the fast electron source. Most of the dimensioning studies for fast ignition targets ignore this stopping power. Even if the fast electron energy deposition in the highly compressed nuclear fuel core is dominated by collisions, it is important to quantify the resistive stopping power in regions closer to the electron source, as this is likely to determine the maximum energy transported by the fast electrons.

2. Experimental results

Our experiment was conducted using the PICO 2000 laser system at LULI. We used long laser pulses (LP) with 180 J, 1.5 ns, 0.53 μm, 500 μm diameter flat-top focal spot at 22.5° angle of incidence (with respect to the target normal axis) to compress the foils by shock-propagation. A counter-propagating high-intensity short laser pulse (SP), with 40 J, 1 ps, 1.06 μm, giving a focused intensity $\approx 5 \times 10^{19}\,\mathrm{Wcm^{-2}}$ at 45° angle of incidence, generated the intense currents of fast electrons which propagated deep into the target. We used foil targets with propagation layers of different thickness (between 10 and 40 μm) of either aluminium (Al) or plastic (CH). All the targets had a 10 μm CH as a generation layer (SP side of the target) and a 10 μm Cu tracer after the propagation layer, followed by 10 μm Al +10 μm CH double layer on the LP side. The results for compressed targets were compared to the uncompressed, solid density targets (interactions without the LP beam). For each target we had previously studied the shock wave generated by the LP beam, in particular its velocity and the time needed to breakout on the SP beam side of the target. This was done by streaked-optical-pyrometry (SOP) of the self-emission from the SP-irradiated side of the target to achieve the correct relative timing of the LP and SP beams such that the compressed length of the target propagation layer was maximised whilst maintaining a cold, solid surface for SP beam interaction [3].

The results of the measurements of Kα emission from the Cu tracer are summarized in Figure 1. We imaged the Cu-Kα emission with a spherical Bragg crystal. From the radius of the signal as a function of the overdense thickness of the target (Fig. 1-a), we deduce a divergent fast electron propagation with a half-angle of $36 \pm 4°$. The abscissa corresponds to the length between the relativistically corrected critical density and the middle of the Cu layer [3]. We do not measure a difference in the divergence as a function of the propagation-layer material, Al or CH, solid or compressed.

The Cu-Kα emission yields are plotted in Fig. 1-b) as a function of the target areal density (again corresponding to the distance from the coordinate of the critical density to the middle of the Cu layer). These yields correspond to the integration of the emission spectral lines measured with a conical Bragg crystal. We see that: i) in solid targets the Cu-Kα signal is stronger for an Al compared to a CH propagation layer; ii) in compressed targets the signal yields for Al and

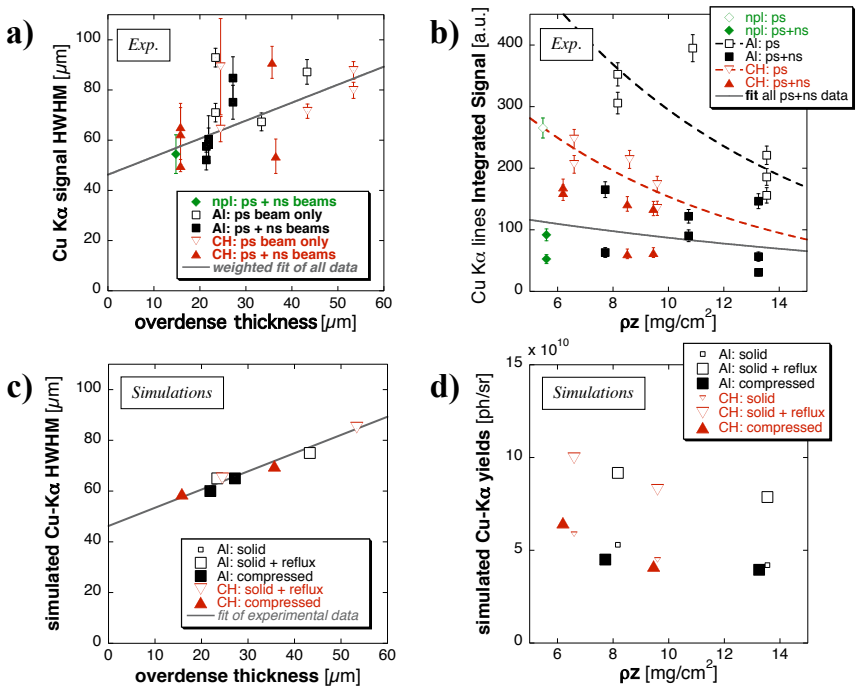

Figure 1. **a)** Experimental radius of the Cu-Kα emission as a function of the targets' overdense thickness. **b)** Experimental Cu-Kα yields as a function of the targets' areal density (the exponential curves fitting the data are plotted only to guide the eye). **c)** and **d)** Numerical equivalents of **a)** and **b)**, respectively.

CH are comparable; iii) signal yields are lower in compressed than in solid targets for both Al and CH propagation layers, the difference being larger in the case of Al.

3. Discussion

Point i) is explained by the electric field inhibition of the fast electron propagation in cold CH layers, as evidenced in previous work [4].

Point ii) is also well understood as both compressed Al and compressed CH propagation layers are partially ionised and behave like conducting plasmas. In fact, 2D hydro-radiative simulations using the code CHIC, accounting for the effects of the LP-induced shock and of the SP ASE-pedestal, showed that both the compressed Al and CH were heated up to $\sim 4\,\mathrm{eV}$ and had comparable densities of free electrons and comparable degrees of ionization.

Hybrid simulations of the electron transport help to understand point iii). The fast electrons source is injected as dictated by a CALDER-PIC simulation of the SP laser beam interaction with the density gradient created by the ASE-pedestal (the pre-plasma density profile was evaluated for $10^{19} < n_e < 10^{20}\,\mathrm{cm}^{-3}$ by side-on interferometry 300 ps before the intense part of the pulse and cross-checked by 2D CHIC hydro calculations [3]). The results from the hybrid transport simulations, including a Kα emission package, are summarized in Figures 1-c) and 1-d). From this first set of simulations, we can appreciate in Fig. 1-c) that the calculated radial width of the Kα emission from the Cu fluorescent layer perfectly reproduces the linear fit of the experimental measurements. In agreement with the experiment, there is no divergence dependence on the propagation-layer material. In Fig. 1-d) the calculated Kα emission yields qualitatively reproduce the experimental trends for the compressed targets (full symbols) but this is not the case for the solid targets (small open symbols).

The higher fluorescence yields measured for the solid targets can only be reproduced if fast

electron re-injection into the target at the unperturbed rear surface is included in the simulations (big open symbols in Fig. 1-d). There is a high probability that these refluxing fast electrons propagate again across the Cu layer, in the opposite direction, raising (approximately doubling) the time-integrated fluorescence yields. This cannot happen in the compressed case, as the LP beam creates a several-100s μm-long and underdense coronal plasma behind the ablation front. We investigated the effect of the refluxing electrons in the hybrid simulations using ideal elastic scattering at the target rear surface. This edge condition is completely artificial, but is justified by PICLS simulations (without collisions) of the fast electron transport including large regions beyond the targets initial limits, thus simulating the electrons trajectories in the front and rear side sheaths. The simulations reveal that after 2 ps, a factor of ~ 2 times more electrons having crossed the Cu fluorescent layer compared to the case without refluxing. This supports the use of the artificial edge-reflection conditions in the hybrid simulations.

Even with electron refluxing we cannot, however, explain the measured differences between Kα yields from solid CH and solid Al targets. We tested the effect of changing the electron source radius and injection angular distribution in the simulations, within the limits for which the resulting Kα signals compare quite well to the experimental data and their error bars. By altering these two parameters, it was found that if the fast electron current density j_h is kept between 10^{10} and $10^{12}\,\mathrm{Acm}^{-2}$ through $15\,\mu$m of material, the electron beam energy loss rate due to collective mechanisms is 10-20% higher in compressed Al than in solid Al at equal depth. This is mostly attributed to the resistivity increase of the compressed Al as it is heated to a temperature close to the Fermi temperature. The difference is relatively small because the resistivity differences exist only for the first 0.8 - 1 ps. This is the time needed for the target bulk to be heated by the fast electron beam to temperatures $> 10\,\mathrm{eV}$, attaining the Spitzer transport regime in either the initial solid or warm-compressed Al, and where no differences are expected between the two cases. For $j_h < 10^{10}\,\mathrm{Acm}^{-2}$, resistive effects are negligible compared to the collisional energy losses. For $j_h > 10^{12}\,\mathrm{Acm}^{-2}$, the rate of collective energy losses increases, but the head of the fast electron beam heats the background material so rapidly that we can practically consider the Spitzer regime as the initial state for both solid and compressed cases.

For the CH targets, the yields of the Kα signal are also weaker for the compressed case compared to the solid case, but the difference is less than for Al - the effects of electron refluxing in the non-compressed case compensates for the effects of the higher resistivity of cold plastic. For our intense interaction regime, producing high current densities, the initial higher resistivity of CH compared to Al is very rapidly cancelled by the fast electrons energy deposition and target heating. This is different to what has been reported in previous work performed in a non relativistic regime [5].

4. Conclusions

We have identified a regime for the fast electron current density, $10^{10} < j_h < 10^{12}\,\mathrm{Acm}^{-2}$, for which differences in the collective transport in solid Al compared to compressed Al are measurable for our experimental conditions. The complete simulated picture of the experiment is ongoing and involves correct modelling of the CH conductivity as a function of temperature and the fast electron source radius as a function of electron energy and time. Nevertheless, our results show the importance of electric field effects, changes in plasma conductivity and insulator-to-conductor phase transitions on fast electron transport in dense matter.

References

[1] Nakamura H *et al.* 2008 *Phys. Rev. Lett.* **100** 165001
[2] Perez F *et al.* 2009 *Plasma Phys. Control. Fusion* **51** 124035
[3] Santos J J *et al.* 2009 *Plasma Phys. Control. Fusion* **51** 014005
[4] Pisani F *et al.* 2000 *Phys. Rev. E* **62** R5927
[5] Hall T *et al.* 1998 *Phys. Rev. Lett.* **81**, 5, 1003